JOURNAL OF AIRCRAFT
Vol. 44, No. 4, July–August 2007

Optimization of Airfoil Flow Control Using a Genetic Algorithm with Diversity Control

Liang Huang,* George Huang,† and Raymond LeBeau‡
University of Kentucky, Lexington, Kentucky 40506-0108
and
Thomas Hauser§
Utah State University, Logan, Utah 84322-4130

DOI: 10.2514/1.27020

The aerospace community is on the verge of a new generation of practical active flow control devices, from synthetic jets to plasma actuators. However, even as the mechanical challenges of implementing these systems seem attainable, the proper placement, orientation, and energy inputs to achieve the maximum benefit in a variety of flow conditions are often poorly known. Successful application of computational fluid dynamics to this type of control problem critically depends on an efficient searching algorithm for design optimization. Based on our previous research of single-suction/blowing-jet control on a NACA 0012 airfoil, the design parameters of a test two-jet system are proposed. A genetic algorithm drives the computational fluid dynamics simulations, guiding the configuration of a suction jet and a blowing jet on the airfoil's upper surface. Reasonable optimum control values are determined within the control parameter range, and the sensitivity of the control values can be determined through a comparison of the fitness value from a large number of computational fluid dynamics simulations.

Nomenclature

A	=	suction/blowing amplitude
C_d	=	drag coefficient
C_l	=	lift coefficient
C_p	=	pressure coefficient
L_j	=	jet location
u	=	x component of the jet entrance velocity
v	=	y component of the jet entrance velocity
β	=	angle between the freestream velocity direction and local jet surface
θ	=	suction/blowing angle between the jet velocity direction and the local jet surface

Subscripts

B	=	baseline case, blowing
S	=	suction

I. Introduction

THE use of evolutionary algorithms (EAs) is now relatively widespread as a tool to optimize complex design spaces. Recent examples of EAs used in conjunction with computational fluid dynamics (CFD) include the design of airfoils [1] and turbine cascades [2]. In these efforts, the evolutionary algorithm has proven an efficient and robust path to optimization. The advantages of an evolutionary algorithm approach should increase as the parameter space becomes increasingly complex, with a growing number of local extrema potentially masking the optimal solution.

One example of a potentially complex design space is the configuration of active flow control systems for airfoils. For example, an array of synthetic jets distributed across an airfoil surface provides the potential for a plethora of arrangements, with varying amplitudes, frequencies, and locations. Methods that rely on wing warping, wing morphing, or plasma actuators similarly present a complex environment in which the optimal combination of parameters is not necessarily obvious. In these cases, a design process that relies on trial and error and the designer's knowledge and intuition may not prove sufficient to cover the wide range of possible flow conditions. Likewise, experimental research will necessarily be limited due to the challenge of creating a new model for each configuration. This leaves computational fluid dynamics, and as computer hardware and computational techniques continue their relentless advance, CFD-driven investigation of airfoil flow has become increasingly detailed and sophisticated. Although many of the apparatus of future active flow control have yet to be practically applied, computationalists are already addressing the challenges of accurate simulations [3]. Still, even with the long-term growth of computer power, it seems improbable that a simply systematic search of a complete parameter space can be completed in a timely fashion.

As such, a promising approach to the design of active flow control systems is the use of CFD in conjunction with EAs. However, a traditional binary genetic algorithm (GA) and its operators are not necessarily the best approach for real-world engineering problems. Representing real design variables as traditional binary strings is but one complication. Another is driving the GA to move more rapidly from a global search to finding near-optimal regions to actual convergence on a fine-grained, more precise optimum when there is a limited time frame and the cost of evaluating a genome's fitness through CFD simulations is high. A third is that complex flow control problems can lend themselves to a variety of local optima that can trap a search algorithm. More problematically, methods that accelerate convergence are generally more susceptible to being trapped in local optima.

The approach taken in this paper is to combine different existing GA techniques into a real-coded explicit adaptive range normal distribution (EARND) genetic algorithm with diversity control. This technique is applied to a test flow control problem on a NACA 0012

Presented as Paper 225 at the 42nd AIAA Aerospace Sciences Meeting and Exhibit, Reno, NV, 5–8 January 2004; received 3 August 2006; revision received 18 October 2006; accepted for publication 29 November 2006. Copyright © 2007 by P. G. Huang, R. P. LeBeau, and T. Hauser. Published by the American Institute of Aeronautics and Astronautics, Inc., with permission. Copies of this paper may be made for personal or internal use, on condition that the copier pay the $10.00 per-copy fee to the Copyright Clearance Center, Inc., 222 Rosewood Drive, Danvers, MA 01923; include the code 0021-8669/07 $10.00 in correspondence with the CCC.

*Graduate Research Assistant, Mechanical Engineering. Student Member AIAA.
†Professor, Mechanical Engineering; currently Professor and Chair, Mechanical and Materials Engineering, Wright State University, Dayton, OH 45435-0001. Senior Member AIAA.
‡Assistant Professor, Mechanical Engineering. Associate Fellow AIAA.
§Assistant Professor, Mechanical and Aerospace Engineering. Member AIAA.

airfoil. The flow control system consists of two jets, one suction and one blowing. In this case, the system is not too complicated so that the search results may be reasonable checked, in this case against previous single-jet CFD studies conducted on the airfoil under the same flow conditions [4]. Although this flow control system is necessarily modest, repeated successful application of the GA serves to demonstrate the long-term potential of this approach to expand as more active flow control systems move from concept to prototype to practical airfoil design and application. The genetic algorithm generates a large number of distinct CFD solutions. Comparing the influence of several control parameters on the fitness function allows us to determine the dominant control parameters for this problem.

II. Optimization of a Two-Jet Flow Control System Using a Genetic Algorithm

A. Flow Control System

The flow control case presented here is built upon the authors' previous work simulating flow control on a NACA 0012 airfoil based on a single jet under conditions of a Reynolds number of 500,000 and an angle of attack of 18 deg [4]. Based on this earlier research, three parameters (Fig. 1) are selected in the investigation: namely, jet location, suction/blowing amplitude, and suction/blowing angle.

The jet width for both suction and blowing is fixed at 2.5% chord length based on a study by Dannenberg and Weiberg [5], who showed that an increase of suction area beyond 2.5% chord length will not increase lift significantly. On the other hand, the 2.5% length is sufficient to allow accurate numerical simulation on moderate grid resolutions. In the numerical investigation, the jet entrance velocity is set to

$$u = A \cdot \cos(\theta + \beta) \tag{1}$$

$$v = A \cdot \sin(\theta + \beta) \tag{2}$$

where θ is the angle between the local jet surface and jet entrance velocity direction. Note that negative θ represents suction and positive θ indicates blowing. Perpendicular suction and blowing correspond to $\theta = -90$ and 90 deg, respectively. The results of the previous research (Fig. 2) indicate that the maximum normalized lift between suction and blowing for a given amplitude have large differences, with the control effects of suction being much stronger than blowing.

Therefore, in the two-jet control system, we will fix the suction amplitude at 0.03 (or 3% of the freestream velocity) and let the blowing amplitude change within 0 to 0.2; in this manner, the suction control effects will not overwhelm the blowing control effects. With suction amplitude so fixed, five design parameters are adopted for the two-jet control system, with the parameter ranges selected as follows:

1) The suction location is $0.05 \leq L_{jS} \leq 0.8$.
2) The suction angle is $-90\,\text{deg} \leq \theta_S \leq 0\,\text{deg}$.
3) The blowing location is $0.05 \leq L_{jB} \leq 0.8$.
4) The blowing angle is $0\,\text{deg} \leq \theta_B \leq 90\,\text{deg}$.
5) The blowing amplitude is $0 \leq A_B \leq 0.2$.

These parameters allow the jets to achieve full angular motion (fixing one as a suction and one as a blowing jet) and most of the lateral range of the airfoil; the only significant a priori restrictions are those placed on the amplitude.

B. Numerical Method

As with the earlier single-jet study, all present computations were performed with the CFD code GHOST, which is an in-house CFD code developed at the University of Kentucky. The code is based on a finite volume structured formulation with chimera overset grids. The QUICK and total variation diminishing (TVD) schemes are applied to discretize the convective terms in the momentum and turbulence equations, respectively; the central-difference scheme is used for the diffusive terms and the second-order upwind time discretization is employed for the temporal terms. This code was tested extensively

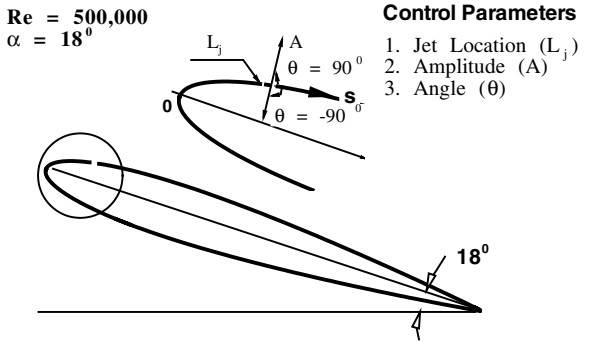

Fig. 1 Control parameters on a NACA 0012 airfoil using suction/blowing control for a single jet.

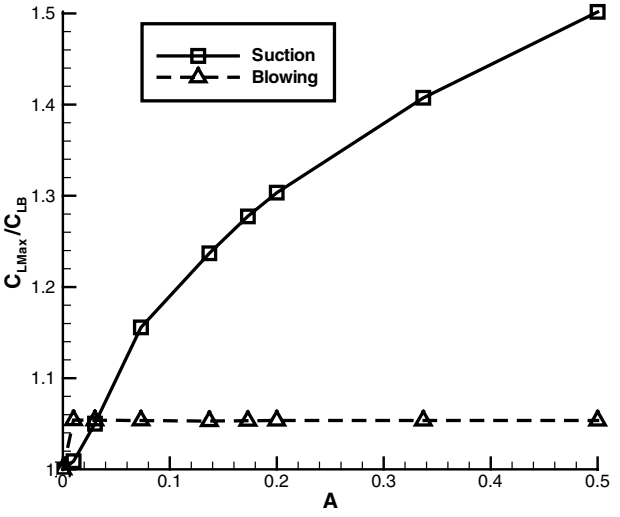

Fig. 2 Maximum normalized lift at different amplitudes of single suction or single blowing of a single-control jet.

and is routinely used for turbulence-model validation [6–8] and flow control studies [9,10], among others. The turbulence model used in the present computation is Menter's [11] shear stress transport (SST) two-equation model, which provides excellent predictive capability for flows with separation. The multiblock and chimera features of the code allow the use of fine grid patches near the jet orifices and in regions of highly active flow. The code also employs distributed memory parallelization using the message-passing interface (MPI) standard [12] to allow different computational zones to be solved on different processors. Current computations are performed on the PC cluster CFDME (64 Intel Xeon 2.66G CPU) and Kentucky Fluid Cluster 2 (48 AMD Athlon 2.0 GHz CPU) at the University of Kentucky.

The Reynolds number being investigated in the present computations is 500,000; therefore, fully turbulent flow with no transition is assumed for the computation. Because the focus of the current investigation is the control of the flow separation through blowing and suction jets, an incompressible Navier–Stokes (N–S) solver is used to eliminate potential additional uncertainties caused by compressibility effects. Previous grid studies on this case [4] have established a grid of 15 overlapping blocks and approximately 210,000 points as reasonably accurate and grid-independent. Further details on these studies may be found in [4,13].

C. EARND Genetic Algorithm with Diversity Control

The basic structure of a genetic search algorithm may now be found in innumerable texts [14,15] and articles, and as such, only a brief introduction is provided here. A detailed description of our basic GA implementation is given in [16]. A GA relies on the variables of interest in the problem being represented as a series of

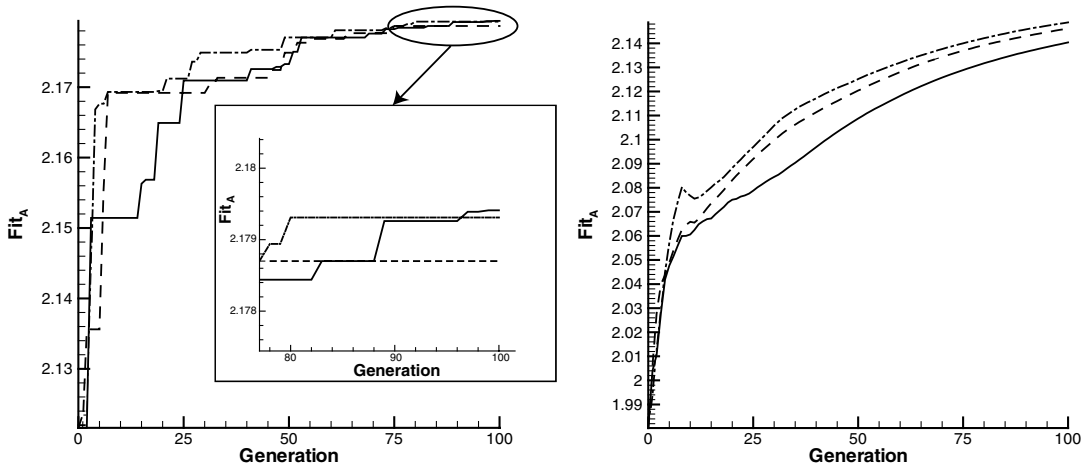

a) Runtime best fitness **b) Offline average fitness**

Fig. 3 Fitness comparison between algorithm without and with diversity control; solid line: with diversity control, dashed line: without diversity control (run 1), dotted-dashed line: without diversity control (run 2).

bits known as a genome, and the overall configuration by a concatenated set of genomes that form an individual. Multiple individuals form a generation, and the generation is allowed to "evolve" by a series of mathematical events that represent effects such as mating (crossover) and mutation. The fitness, again represented by a mathematical function (and in the case of the two-jet flow control study case, linked to the output of a CFD simulation), of each individual is evaluated, and the most fit individuals have the greatest likelihood of passing through to the next generation. Many successive generations are computed, and the individuals corresponding to the most fit solutions (which are not necessarily found in the final generation) are retained as the optimized configuration.

To improve the performance of the search algorithm, three major modifications are made to the base algorithm [13]. First, we add a normal distribution function [17] to act as a global optimization monitor and to speed up the search convergence. Second, in the latter half of the evolution, the search boundaries are explicitly updated to hasten convergence. Third, diversity control is added to the first part of the evolution to reduce the probability of early convergence to a nonglobal optimum. These three modifications are combined with a real-coded GA to create the EARND algorithm with diversity control.

In this paper, the two-jet control system evolution serves a dual purpose. First, it serves as a realistic test of the GA optimization process, specifically, testing the value of diversity control in conjunction with the EARND algorithm on the two-jet, five-parameter control system. Second, the resulting optimum solution provides insight into the flow properties and physics of the two-jet flow control system. A comparative analysis between the one-jet and two-jet simulations serves to confirm the accuracy of the two-jet results and clarifies the important features of these flows.

D. EARND Algorithm Performance with and Without Diversity Control

For the current one suction-jet and one blowing-jet system, three optimization evolutions are completed, each involving 100 generations. The first and second time, the improved genetic algorithm without diversity control is applied; the third time, diversity control is added to the EARND algorithm. The genetic algorithm uses the following parameters: 100 generations, 32 individuals (CFD simulations) per generation, and 5 optimization variables.

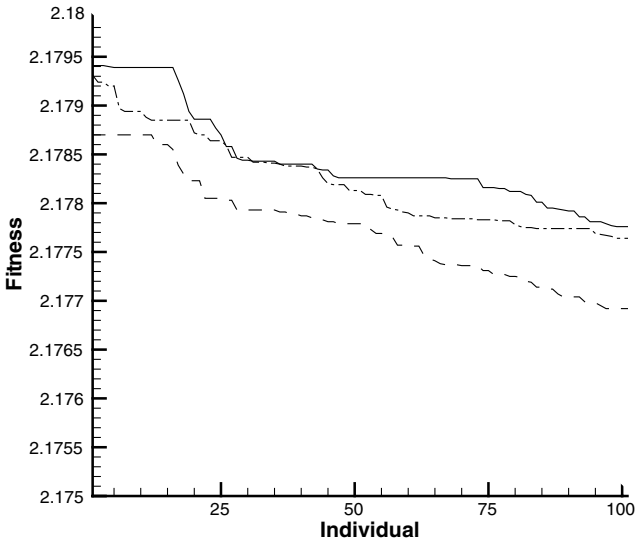

Fig. 4 Fitness of the best 100 individuals using diversity control and no diversity control; solid line: with diversity control, dashed line: without diversity control (run 1), dotted-dashed line: without diversity control (run 2).

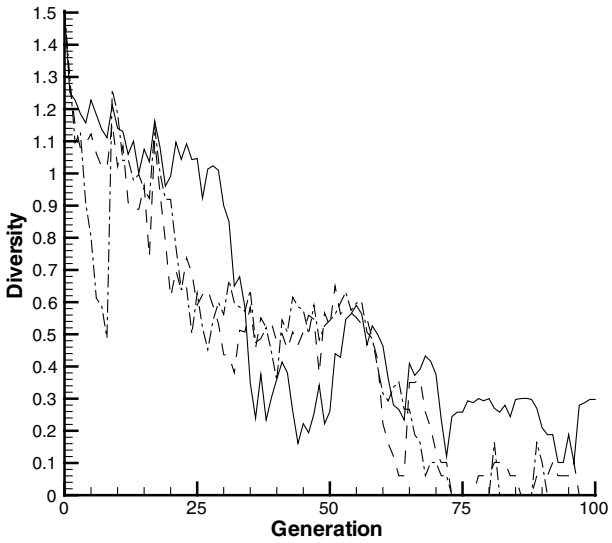

Fig. 5 Diversity level for the algorithm with and without diversity control; solid line: with diversity control, dashed line: without diversity control (run 1), dotted-dashed line: without diversity control (run 2).

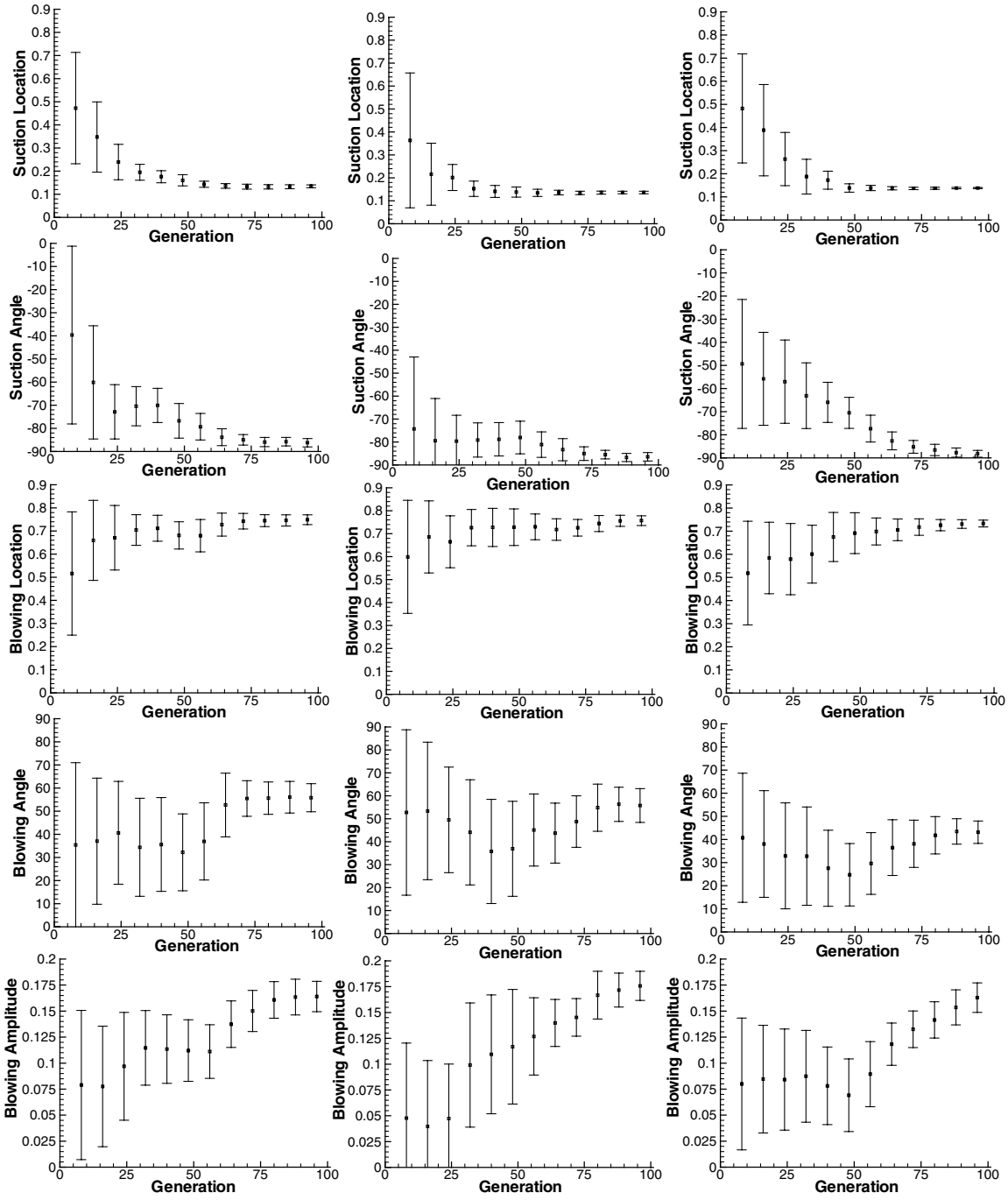

a) Algorithm without diversity control (run 1) **b) Algorithm without diversity control (run 2)** **c) Algorithm with diversity control (run 3)**

Fig. 6 Mean and standard deviation (error bar) of the five GA control parameters.

The system aggregate fitness function is

$$(\text{fit}_A)_{\max} = a \cdot C_l/C_{lB} + b \cdot C_{dB}/C_d \tag{3}$$

where $a = 1.0$ and $b = 1.0$ for the cases tested in this paper. The values $C_{lB} = 0.875904$ and $C_{dB} = 0.166208$ refer to the baseline lift and drag from the equivalent simulation without any jets. The five control parameters (suction location L_{jS}, suction angle θ_S, blowing location L_{jB}, blowing angle θ_B, and blowing amplitude A_B) are optimized by the genetic algorithm toward the maximum aggregate fitness value. Of course, the combination of lift and drag effects can be changed by adjusting a and b values to address the different importance of lift and drag for a given search. For brevity, in the following discussion, "fitness" will refer to "aggregate object fitness."

In Fig. 3, both runtime best fitness and offline average fitness of three optimization evolutions are plotted. Runtime best fitness is defined as the maximum fitness yet achieved among all the individuals up to and through the current generation. Similarly, offline average fitness is the average fitness of all individuals up to and through the current generation. The 0th generation for each evolution starts with 32 individuals constructed of combinations of the maximum and minimum values for each variable, and the initial conditions are the same in all three evolutions. It can be seen from Fig. 3b that the offline average fitness of the algorithm with diversity control is consistently lower than those using the algorithm without diversity control, and similarly from Fig. 3a, that the runtime best

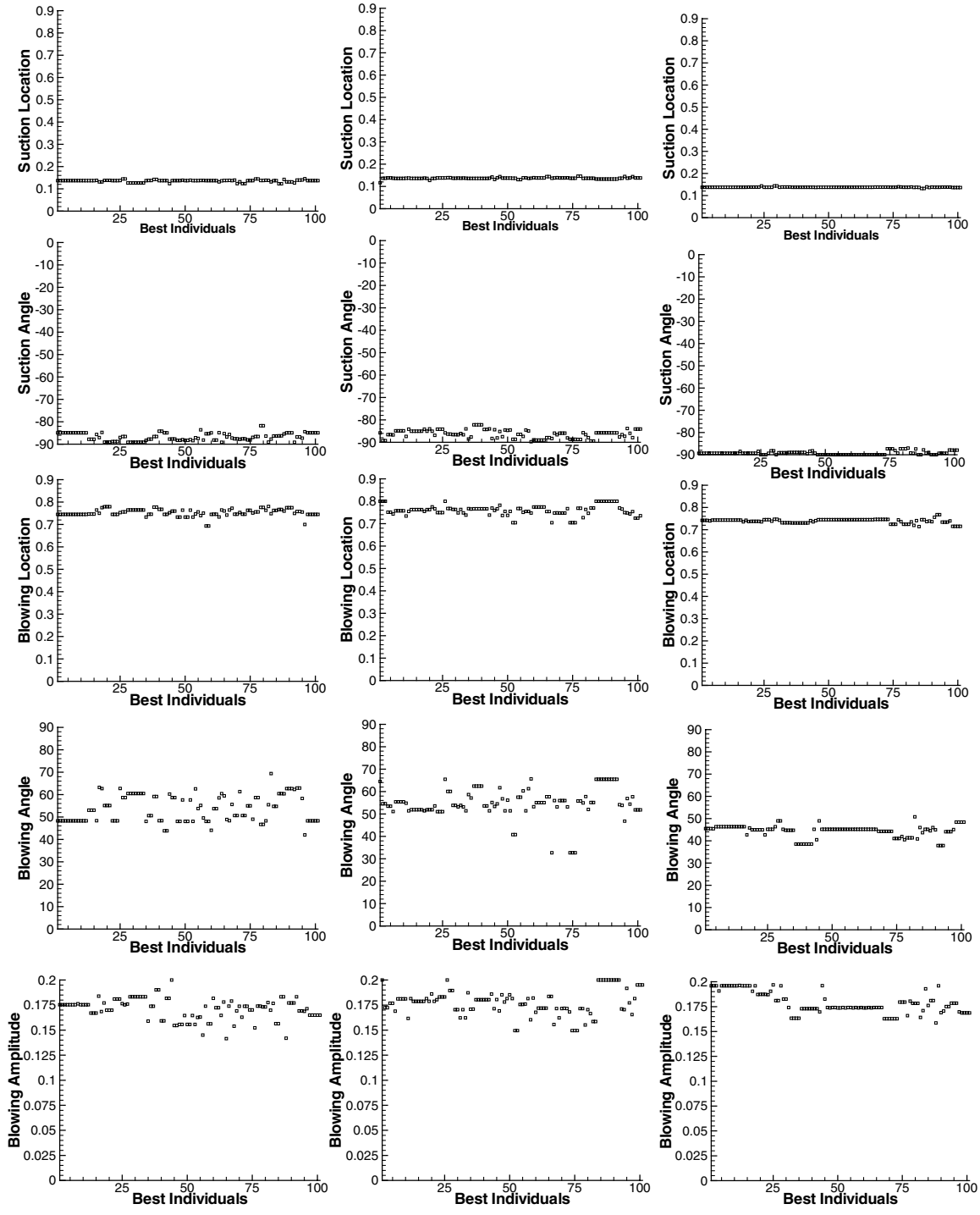

a) Algorithm without diversity control (run 1) **b) Algorithm without diversity control (run 2)** **c) Algorithm with diversity control (run 3)**

Fig. 7 Values of the five GA control parameters for the 100 fittest individuals.

fitness of the diversity-control case lags over the first 20 generations. This is because of the diversity control forcing the first 20% of the evolution away from converging quickly on local optima, an effect that quickly vanishes once diversity control ends in the best runtime fitness but that persists in the running average fitness. In the end, the runtime best fitness of the algorithm is better (although only marginally so) than that of the algorithm without diversity control.

This can also be observed in Fig. 4 by comparing the object fitness of the best 100 individuals generated by each evolution, in which the evolution with diversity control generates the superior outcome throughout.

For the two-jet evolution, the diversity value of each generation is calculated based on a space classification in which each dimension (parameter) is equally divided into two groupings. Therefore, for this five-parameter optimization case, the searching space is divided into 32 categories. From Fig. 5, we can see that the diversity level of the algorithm with diversity control maintains a higher level than the algorithm without diversity control during the initial optimization process, but drops rapidly as the effects of the diversity control wear off. In the final stages of the evolution, the diversity-control case still maintains a higher diversity level, suggesting that even here the search space is more robustly investigated.

Table 1 Optimization run 1 without diversity control

Rank	fit_A	L_{jS}	Θ_S	L_{jB}	Θ_B	A_B	C_l/C_{lB}	C_{dB}/C_d
1	2.178696	0.136	−84.905	0.745	48.305	0.175	1.043	1.134

Table 2 Optimization run 2 without diversity control

Rank	fit_A	L_{jS}	Θ_S	L_{jB}	Θ_B	A_B	C_l/C_{lB}	C_{dB}/C_d
1	2.179307	0.116	−85.766	0.800	64.468	0.200	1.030	1.148
2	2.179241	0.136	−89.233	0.800	54.588	0.172	1.045	1.134
3	2.179201	0.137	−86.567	0.750	53.446	0.176	1.042	1.136
4	2.178975	0.136	−86.706	0.743	51.067	0.168	1.043	1.135
5	2.178944	0.136	−84.846	0.757	55.420	0.181	1.040	1.138

Table 3 Optimization run 3 with diversity control

Rank	fit_A	L_{jS}	Θ_S	L_{jB}	Θ_B	A_B	C_l/C_{lB}	C_{dB}/C_d
1	2.179407	0.137	−89.306	0.742	45.473	0.196	1.043	1.136
2	2.179402	0.138	−89.300	0.740	45.446	0.191	1.043	1.136
3	2.179390	0.137	−89.307	0.743	46.309	0.196	1.042	1.137

In each two-jet control system optimization, every eight generations the new generation will be generated according to the best 256 individuals' statistic information; their means μ and deviation σ are plotted in Fig. 6. In the application, both the lower and upper boundaries are explicitly updated as $\mu - 5.0\sigma$ and $\mu + 5.0\sigma$ in every eight (N update) generations after the 50th generation to cut out unnecessary evaluation in less promising areas. This makes the optimization advance in a more deterministic direction in the second half of the evolution. This is broadly seen in differences in the standard deviation range and the movement toward the optimal regions of the parameter space after the 48th generation in Fig. 6. Through the previous single-jet study, it is known that suction control effects are much stronger than blowing control effects. The main efforts of the optimization process before the 48th generation appear to focus on optimizing suction location L_{jS} and suction angle θ_S to their near-optimum position, whereas the optimization process after the 48th generation seems to emphasize blowing locations L_{jB}, blowing angles θ_B, and blowing amplitudes A_B.

Diversity control appears to slow the convergence of the suction variables initially, reflected in the larger deviation range in generations 16–48. However, by generation 64 the three cases are largely indistinguishable in these three variables, whereas for the suction angle, the range is actually slightly less for the diversity-control case in the last several generations (and is centered about a superior value, as will be seen later). The effect of diversity control is most noticeable in the two least constrained variables: blowing angle and amplitude. Further examining the process before the 48th generation, we can determine that the suction location moves to a near-optimum position faster than the suction angle, which implies that suction location is the more sensitive and thereby more critical parameter. This supposition will be confirmed by the subsequent examination of the flow physics. The process after the 48th generation first moves the blowing location to its near-optimum value and then identifies the near-optimum values of the blowing angle and blowing amplitude. It can be seen that even at the 96th generation, the variances of the blowing angle and blowing amplitude are still considerably larger than the other three parameters (suction location, suction angle, and blowing location). Therefore, we suspect that blowing angle and blowing amplitude are the least sensitive and likely least important parameters for influencing the fitness function among the five control parameters.

In Fig. 7, the five control parameters for the 100 most fit individuals among the 100 generations are plotted in sequence according to their fitness ranking. From this figure, it first can be seen that the solutions scatter across a range instead of converging on some deterministic value, which is expected due to the statistical nature of the genetic algorithm approach. Second, the values for suction location, suction angle, and blowing location scatter less than blowing angle and blowing amplitude. This suggests that for the two-jet control system, suction location, suction angle, and blowing position are the dominant factors in maximizing the aggregate fitness value. Third, the values of all five control parameters of the best 100 fit individuals of the algorithm with diversity control cluster more narrowly than the algorithm without diversity control, another confirmation that early increased diversity can lead to a more converged solution. Because these same individuals are plotted in Fig. 4, the results with diversity control also correspond to superior fitness outcomes.

III. Flow Control Physics

The values for the best individuals from each of the three optimization runs are listed in Tables 1–3. The first and second runs use the EARND genetic algorithm without diversity control; the third run uses the EARND genetic algorithm with diversity control. Although there are some differences between the results (in particular, in the blowing parameters), the basic arrangement (a near-

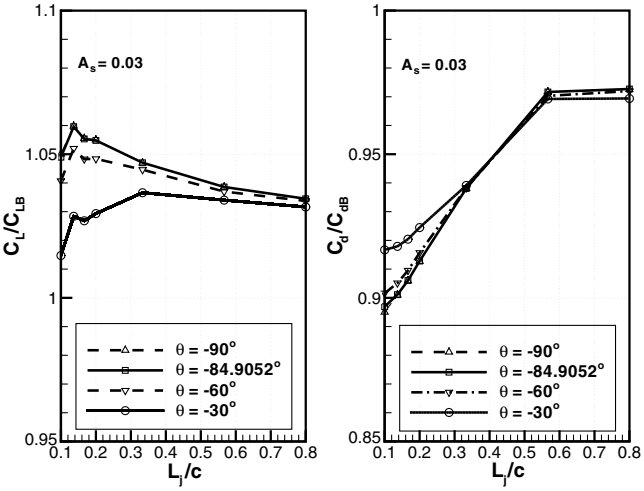

a) Normalized lift **b) Normalized drag**

Fig. 8 Normalized lift and drag for different suction angles along the cord length of the airfoil.

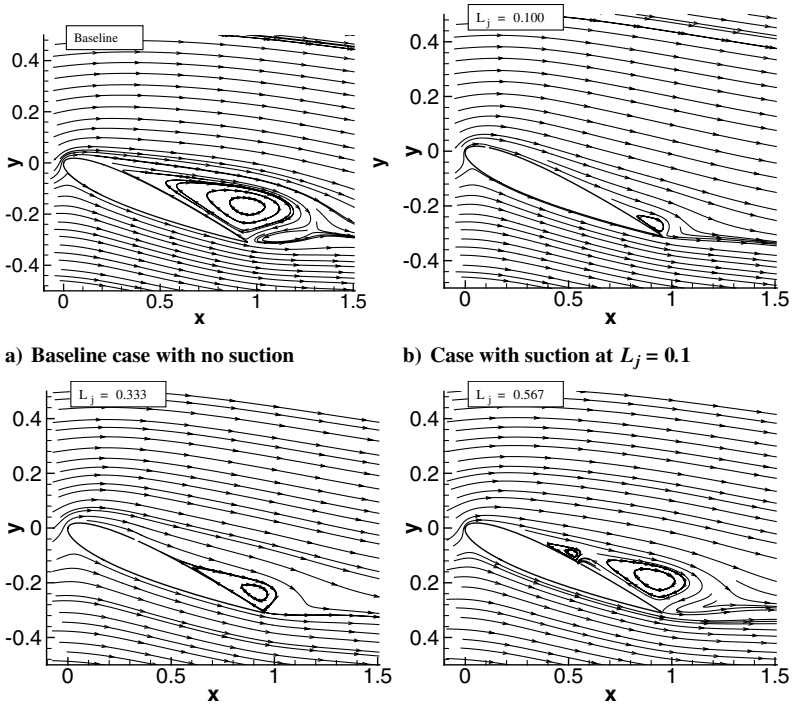

a) Baseline case with no suction

b) Case with suction at $L_j = 0.1$

c) Case with suction at $L_j = 0.333$

d) Case with suction at $L_j = 0.567$

Fig. 9 Effect of suction location on the separation bubble on the airfoil.

normal suction jet at 10–15% of chord behind the leading edge and a downstream jet at 74–80% of chord at an angle of 45 to 55 deg and approaching maximum amplitude) are consistent across all three runs. Therefore, our initial focus will be on the flow control physics for the end results of evolution 1, with further discussion of evolutions 2 and 3 when there are notable differences.

The best individual with the maximum aggregate fitness of 2.178696 after 100 generations of run 1 has the following optimum values: $L_{jS} = 0.136512$, $\theta_S = -84.9052$ deg, $L_{jB} = 0.745153$, $\theta_B =$ 48.3057 deg, and $A_B = 0.175368$. To compare this result with the previously published single-jet study, the discussion of the optimum result is split into suction and blowing components, which will be discussed in the following sections. Given the dominant role of suction in the single-jet studies, the suction jet will receive our attention first. The mechanisms for boundary-layer separation on a thin airfoil and localized suction control measures are described by Degani et al. [18].

A. Suction Control

In Fig. 8, control effects are explored by changing the angle ($\theta_s = -90, -84.9052, -60$, and -30 deg) and position ($L_{jS} = 0.1$, 0.136512, 0.166667, 0.2, 0.333, 0.567, 0.8) and keeping the suction amplitude $A_S = 0.03$ fixed. Here, only suction is applied to the airfoil.

First, considering the suction-angle control effects, the performance at -90 deg suction and -84.9052 deg suction are almost the same (with -90 deg suction slightly better than -84.9052 deg), and both are better than -60 and -30 deg suction. It can be seen that the suction angle of the optimized result of run 3 in Table 3 is -89.3 deg, which is closer to the single-jet optimum of -90 deg. This strongly suggests that the optimum orientation of the suction jet is approaching normal to the surface. Second, the control performance for leading-edge locations are better than those on the airfoil downstream area, and among the seven suction locations, suction at location 0.136512 is better than all other locations. Although the likely reduction in performance from moving the suction jet further downstream is self-evident, the $L_{jS} = 0.1$ case shows that moving it much further upstream will also reduce performance. These two observations are consistent with a previous single-suction-jet study [4], in which the conclusion regarding the suction is that for a fixed suction amplitude comparable to $A_S = 0.03$, perpendicular (-90 deg) suction near the leading edge is most effective. Figure 8 also allows an assessment of the relative importance between the suction location and suction angle. For both normalized lift and normalized drag, the greater effect is achieved by changing suction location than suction angle; in other words, the flow is more sensitive to the suction location than to the suction angle. This confirms our previous analysis of Figs. 6 and 7, in which suction location converges faster and clusters more densely than suction angle.

The critical role of suction location can be clearly seen in Fig. 9. In this figure, the -90 deg suction amplitude is 0.173 (or about six times greater than 0.03) to more clearly demonstrate the suction-control physics.

The flowfields are compared with the baseline case (without suction and blowing). The streamlines of these three suction cases all demonstrate a smaller separation bubble on the surface of the airfoil than the baseline case. In Fig. 9b, when suction is applied near the

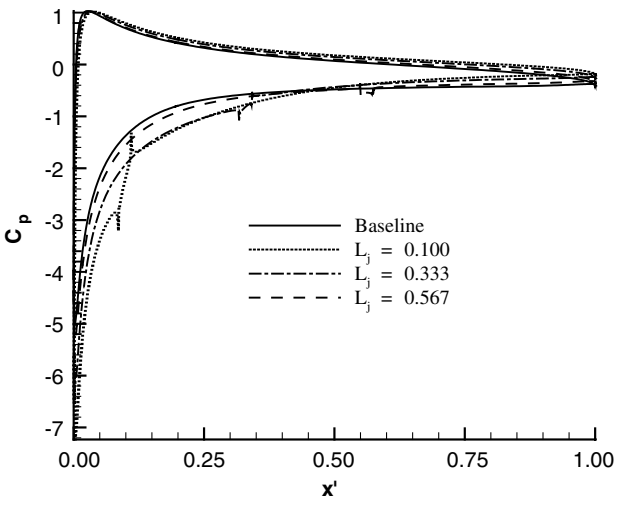

Fig. 10 Influence of suction location on C_p.

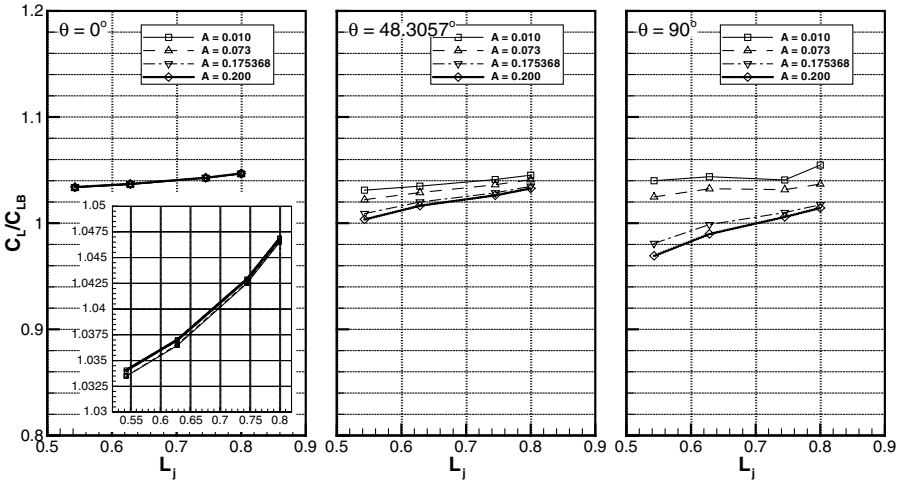

a) Influence of blowing on C_l

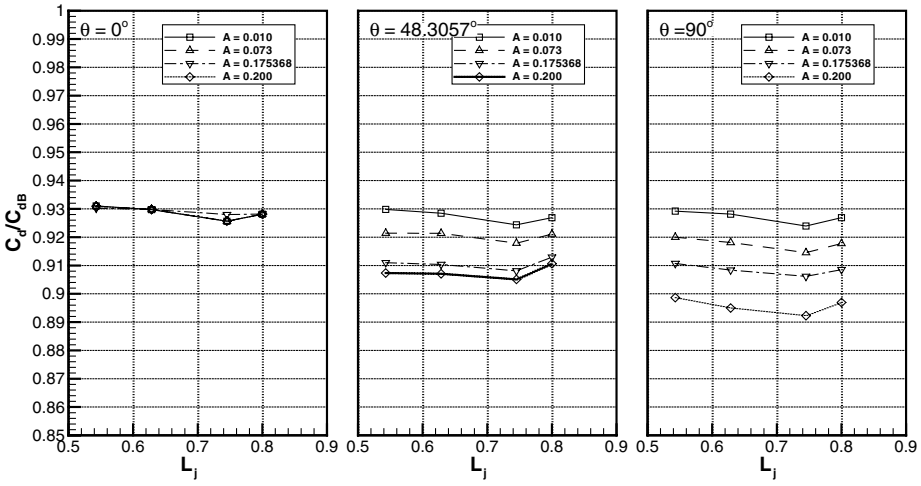

b) Influence of blowing on C_d

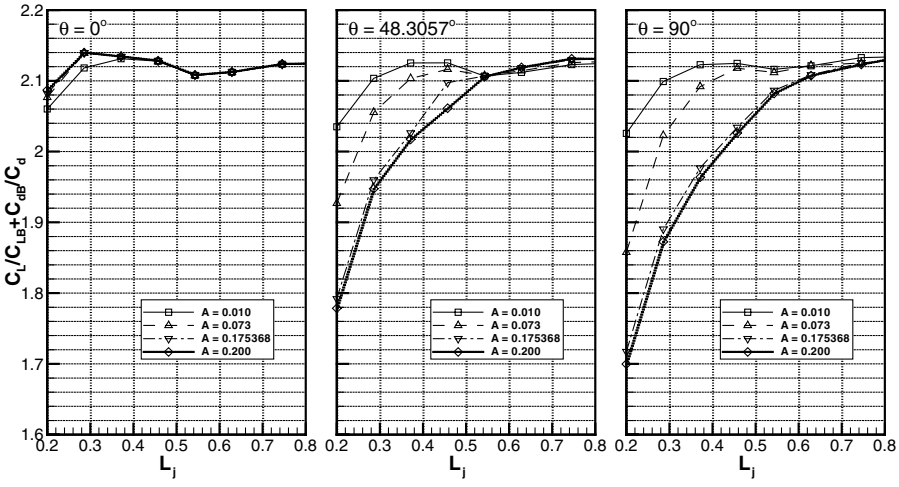

c) Influence of blowing on the fitness function

Fig. 11 Influence of the location, angle and blowing strength on lift, drag, and the fitness function of the GA.

leading edge ($L_j = 0.1$), the separation is most effectively delayed and hence the separation bubble is much smaller than in the other cases. At $L_j = 0.567$, the only control effect of suction is to break the separation bubble into two smaller separation bubbles, and its lift increase is less than that for suction at location 0.1. It can be observed from Fig. 10 that the pressure change near the leading-edge area is significant, and leading-edge suction changes the upper-surface low-pressure zone more efficiently than downstream suction. From this

Table 4 Parameter study of the two-jet control system with different conditions

Rank	fit_A	L_{jS}	Θ_S	L_{jB}	Θ_B	A_B	C_l/C_{lB}	C_d/c_{dB}
*	2.178696	0.136	−84.905	0.745	48.306	0.175	1.044	0.881
1	2.169728	0.136	−84.905				1.060	0.901
2	2.129775			0.745	48.306	0.175	1.029	0.908
3	2.170408	0.137	−84.905	0.745	0.000	0.175	1.059	0.900
4	2.174480	0.137	−84.905	0.745	90.000	0.175	1.025	0.870
5	2.179974	0.137	−84.905	0.745	48.306	0.200	1.041	0.878
6	2.179061	0.137	−90.000	0.745	48.306	0.175	1.044	0.881

figure, it can be seen that the underlying suction control mechanism is the suppression of the separation bubble and the reduction of the airfoil upper surface C_p to increase lift and decrease the profile drag.

B. Blowing Control

The blowing control parameters from the best two-jet solution from optimization run 1 are $L_{jB} = 0.745153$, $\theta_B = 48.3057$ deg, and $A_B = 0.175368$. The control effects of these three blowing parameters are explored and compared with the results of our previous single-blowing-jet study in Fig. 11. The values of the three blowing parameters being explored are $L_{jB} = 0.542857$, 0.628571, 0.745153, and 0.8; $\theta_B = 0$, 48.3057, and 90 deg; and $A_B = 0.01$, 0.073333, 0.175368, and 0.2.

First, from Fig. 11a, it can be seen that for downstream blowing with fixed blowing location and blowing amplitude, tangential blowing is insensitive to amplitude changes and has a larger impact on increasing lift than other angles. Second, the results from Fig. 11b also indicate that downstream locations 0.745153 and 0.8 are better for increasing lift. These two locations are both reflected from the blowing location part of the optimized results in evolutions 1, 2, and 3. Another important observation in Fig. 11 is that the control effects generated by the nontangential blowing jets actually reduce both lift and drag with increasing amplitude, indicating a potential design tradeoff. As such, downstream tangential (0 deg) blowing seems more advantageous at most of the locations, with the exception at around 0.8, in terms of increasing lift. For all three angles tested, a relatively small ($A_B = 0.01$) amount of downstream blowing can generate significant lift enhancement of about 4%. Like lift, drag reduction is insensitive to amplitude for tangential blowing, and a small amount of blowing can generate significant drag reduction (about 7% at $A_B = 0.01$), but unlike lift, drag characteristics benefit from larger amplitude for nontangential angles. However, these lift–drag tradeoffs with amplitude are not simply proportional. As such, the blowing-jet configuration of maximum fitness is an intermediate state between that of maximum lift (tangential blowing, low amplitude) and minimum drag (perpendicular blowing, high amplitude). Drag also exhibits a local minimum around $L_{jB}=$ 0.74515, consistently across all angles and amplitudes. Fitness has a clear sensitivity with location, with maximum fitness occurring downstream, but varies in a more complex fashion with blowing angle and amplitude. At the moderate angles selected by the GA-CFD evolutions, increasing amplitude does seem to lead to improved performance, with a flattening of the curve as $A_B = 0.2$ is approached.

C. Two-Jet Control

Because the suction is the dominant control factor, comparing the two-jet optimized results with the single-suction/blowing-jet results not surprisingly yields the optimized locations in a tight region near the leading edge (0.136512 in run 1, 0.116531 and 0.136901 in run 2,

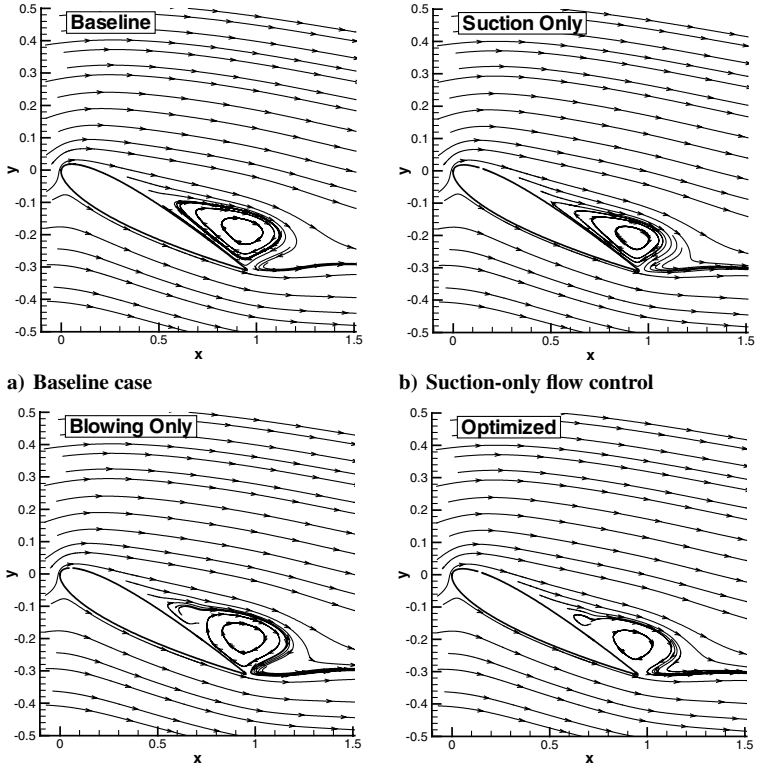

a) Baseline case b) Suction-only flow control

c) Blowing-only flow control d) Optimized two-jet flow control system

Fig. 12 Effects of different flow control approaches on separation on a airfoil.

and 0.137383 in run 3) and nearly perpendicular suction angles (−84.9052 deg in run 1, −85.7663 deg in run 2, and −89.3069 deg in run 3), both of which are generally consistent with the optimal single-jet results. For the blowing jet, as seen in the single-jet results, the GA appears to have selected a configuration that yields optimal fitness between that for maximum lift and that for minimum drag. The optimized blowing locations of 0.74515 in run 1, 0.8 in run 2, and 0.741999 in run 3 are in the range of optimal locations suggested by single-blowing-jet studies. The effect of blowing angle and amplitude on fitness is less sharply defined than that of location. As such, the GA is less sensitive to their precise convergence to a local maximum. This is suggested by the relatively small increase in aggregate fitness (only about 20% of the overall improvement) in the second half of the evolution.

To examine the sensitivity of the two-jet control system to each parameter, different conditions relative to or within the vicinity of the best optimized results are explored, and their normalized lift, normalized drag and aggregate fitness are listed in Table 4.

Figure 12 shows the effect of the previously discussed flow control approaches on the separation bubble size, and Fig. 13 shows the corresponding pressure coefficients. The baseline case, shown in Fig. 12a, has the largest separation region shown by the streamlines. The smallest separation is the suction-only case [Fig. 12b, whereas the blowing-only (Fig. 12c) and two-jet system cases (Fig. 12d) seem to have similar separation sizes].

First, from the flow patterns in Fig. 12, comparing the suction-only case (run 1, Fig. 12b) to the baseline (no blowing/suction, Fig. 12a) case, it can be seen that the suction increases lift and decreases drag by suppressing the separation bubble. Second, comparing the blowing-only case (run 2, Fig. 12c) to the baseline case, it is clear that the physical effects are more subtle than those due to suction. The earlier single-blowing control study [4] demonstrates that blowing increases lift and decreases drag through increased circulation, although the control effects are much less than suction, given larger amplitude conditions. However, there may be additional physical effects that characterize blowing in this two-jet configuration. Third, comparing the two-jet optimal GA solution (case *) to the baseline case, the separation bubble is reduced by the suction; on the other hand, the circulation about the separation bubble is expected to increase due to the downstream blowing. These changes are reflected in the surface pressure coefficient (C_p) changes in Fig. 13, and it can be seen that the C_p value of the optimized case is slightly higher than the suction case due to the blowing-jet effects.

Further examining Table 4, it can be seen from the normalized lift and normalized drag changes that the optimized two-jet control system from run 1 (case *) can be imagined as a best single-suction system (case 1) combined with an appropriate blowing system (case 2). When blowing effects are stacked on the suction effects, normalized drag decreases more than normalized lift decreases, and so the combination of suction and blowing yields a better total aggregate fitness, although the net effect is not large. To investigate the blowing-angle parameter, cases 3 and 4 in Table 4 change only the blowing angle from case *. In both cases, the aggregate fitness is less than the optimized case; it can be seen that from the 0-deg blowing angle of case 3 to the 90-deg blowing angle of case 4, both normalized lift and normalized drag decrease. This implies that the optimal solutions of 45–55 deg over the three evolutions are a compromise between two potential extremes picked out by the genetic algorithm. Cases 5 and 6 likewise study the sensitivity of the GA. In case 5, the blowing amplitude is increased to the maximum possible value of 0.2; in case 6, the suction angle is decreased to the minimum (and the ideal single-jet value) of −90 deg. Both of these cases yield a slightly greater aggregate fitness than case * (optimum result of run 1). Therefore, the optimum result in run 3 is probably closer to the true optimum result, a probable consequence of the addition of diversity control.

However, although the genetic algorithm approach may be able to select an optimum design to the *n*th decimal place, a more realistic assessment of the results requires consideration of the accuracy of the CFD simulation relative to a real system and the reasonable expectation of precision that a practical flow control application can

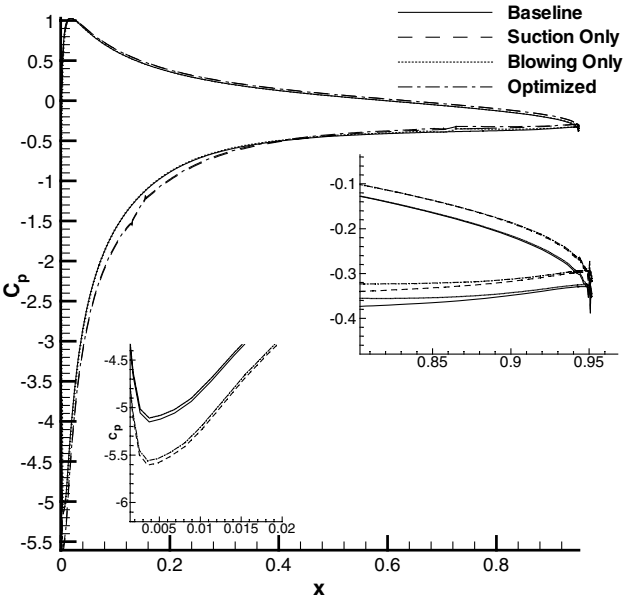

Fig. 13 Pressure coefficient C_p for the NACA 0012 airfoil.

achieve. References [3,19] investigated the gap between the ideal expected performance and actual performance in experimental flow control applications, as well as the ability of current CFD practices to match flow control results. The combined results suggest that at this stage, a degree of caution must be exercised in evaluating flow control simulation. Further, the high precision of the EA result is less relevant in terms of applications in which locating a jet a few inches further forward to avoid structural weakness might be more critical than a 0.01% increase in the generated lift.

Because this test case does not represent an actual system, it is not possible to directly validate these proposed optimal solutions, although in the preceding sections, we have made the effort to demonstrate that the results are at least physically reasonable and consistent with earlier CFD studies. An alternate approach to account for potential errors and construction limitations is to consider all the configurations that fall within a certain error limit of the maximum fitness value and then determine the range of each parameter that is encompassed within these possible solutions; such plots are shown in Figs. 14 and 15. Figure 14 combines results from all three evolutions with a fitness value within 0.5% of the maximum fitness value from evolution 3 or fitness values above 2.1685.

Figure 15 does the same for evolutions within 1.5% or fitness values above 2.1467. To provide perspective, a variation of 0.5% in a lift result is often considered sufficient to demonstrate CFD grid independence between two difference grid refinements; 1.5% error in many instances could be considered acceptable error when comparing the CFD simulation and experimental results. This second range also allows for further error due to the fact that the computation may not precisely mirror reality or, as often as not, reality cannot be accounted for or measured with this degree of numerical rigor in reasonably complex flows. In the 1.5% case, more than half of the 3200 individuals evaluated in the total evolution qualify for inclusion, indicating that many of the CFD computations were quite similar in form.

From these results, it is apparent that the suction jet should be located toward the leading edge for even moderate improvement in the fitness value. The suction angle and blowing location are strongly constrained within the 0.5% error case and moderately constrained within the 1.5% error case, with a near-normal suction angle and downstream (between 70–80% of the chord) blowing location. Conversely, the blowing amplitude is more weakly constrained, although the results suggest that blowing amplitudes greater than 0.15 but less than 0.19 are probably preferable. The blowing angle is hardly restricted at all, with the reasonable solutions primarily occurring between 30 and 70 deg.

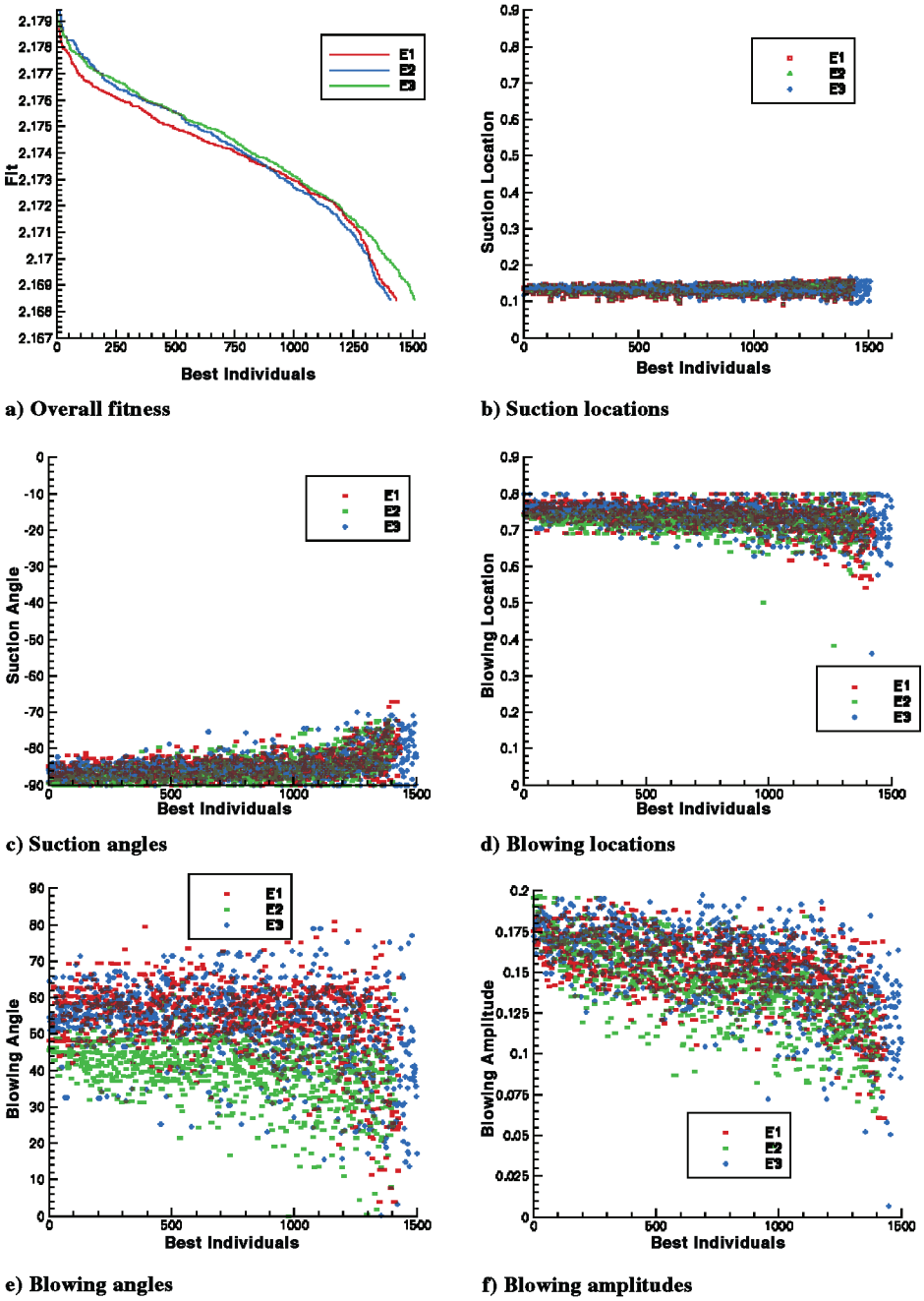

Fig. 14 Overall fitness and distribution of the five optimization parameters for all individuals within 0.5% of the best fitness from all three evolutions.

An implication of these results, besides stressing the relative unimportance of the blowing-jet angle and amplitude within the given parameters, is that the jet problem may be better served by multiple, shorter evolutions rather than fewer, longer ones. As seen in Fig. 6, in which the mean and 5σ normal distribution at each N update generation are shown for the three runs, the last 50 generations of these evolutions primarily served to define blowing-jet amplitude and angle, effectively tweaking these parameters to yield the marginal fitness improvements seen in Fig. 3. It is therefore possible that a more advantageous approach would be to conduct two 50–60 generation evolutions, with the first 20 generations using diversity control and the last 20 using accelerated convergence, rather than a single 100-generation approach. The tradeoff would be a reduction in searching for a precise, resonancelike configuration that yields significant improvements within a precisely narrow range of parameters. However, given the preceding arguments, such a narrowly tailored solution may be beyond the accuracy of the CFD code or may just not be practical to implement in real-world systems to the necessary degree of precision.

IV. Conclusions

A GA was applied to optimize a two-jet flow control system on an airfoil. Analyzing the two-jet GA solution in detail reveals that the suction jet is dominant and the blowing jet is secondary to the overall fitness improvement, even with the blowing amplitude being six times that of the suction. This is consistent with previous studies of the single-jet flow physics. Based on the results, the most important and fastest converging parameters are the suction location and angle. The blowing location is of secondary importance, although the blowing angle and blowing amplitude are the parameters least well-constrained and least critical to the overall performance of the two-jet

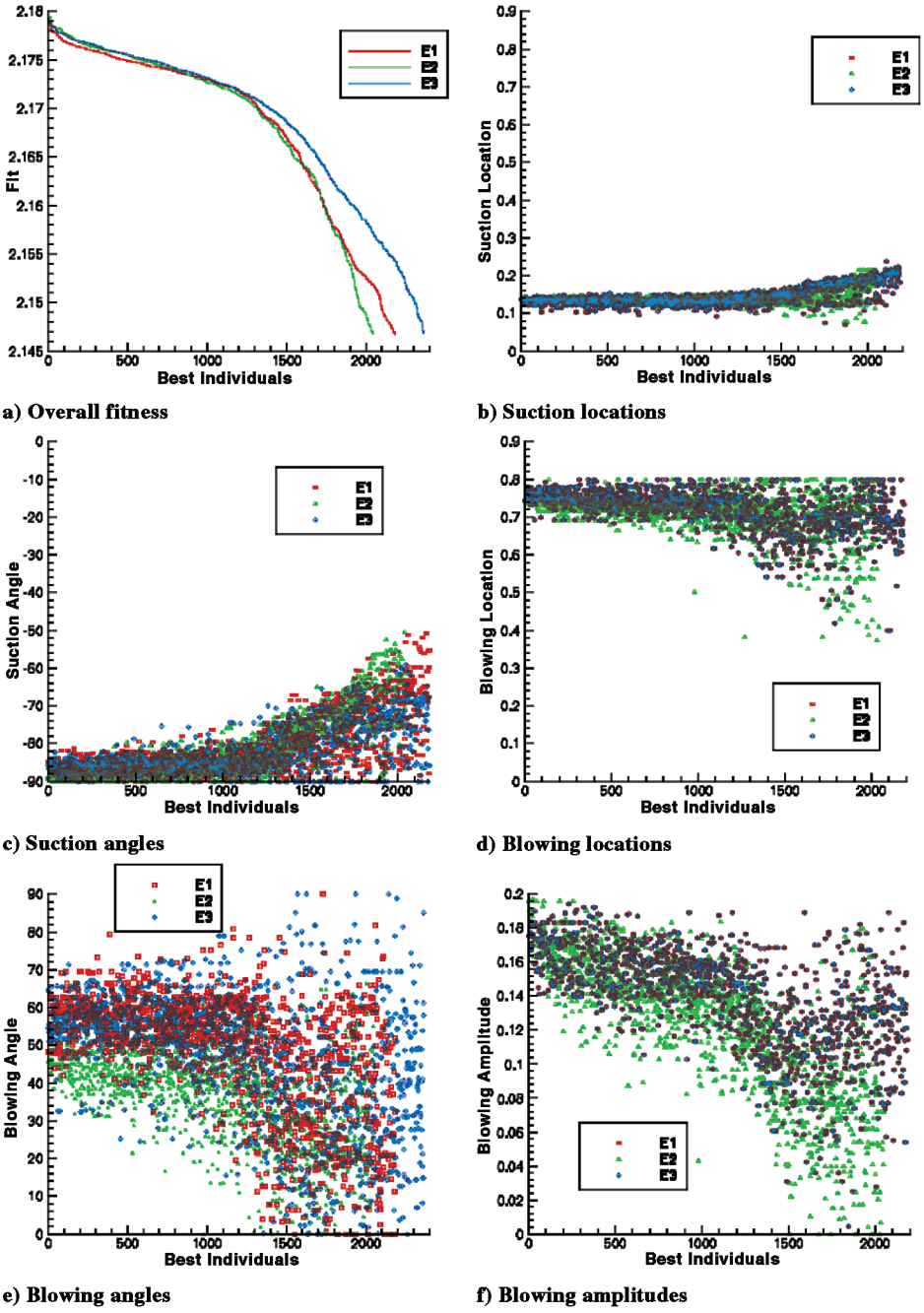

Fig. 15 Overall fitness and distribution of the five optimization parameters for all individuals within 1.5% of the best fitness from all three evolutions.

system. All three evolutions yielded a basic configuration of a near-leading edge, near-perpendicular suction jet, with a downstream blowing jet at a moderate angle and relatively high amplitude. The consequential weakening of the separation bubble is the physical explanation for the increased lift and decreased drag due to the jets.

Of course, the preceding jet analysis is only as good as the underlying simulations, and the many-digit precision of the genetic algorithm parameters is excessive. We do not claim as a practical matter that the optimum configuration of evolution 1 being 0.032% worse than that of evolution 3 is significant. But the GA-CFD combination did determine a clear general configuration that was optimal by a significant amount (9% fitness gain over the baseline case) and which was consistent with previous single-jet results. This demonstrates the potential for combining evolutionary algorithms with computational fluid dynamics to investigate more complicated flow control systems.

References

[1] Gonzalez, L., Whitney, E., Srinivas, K., and Periaux, J., "Optimum Multidisciplinary and Multi-Objective Wing Design in CFD Using Evolutionary Techniques," *Computational Fluid Dynamics 2004: Proceedings of the Third International Conference on Computational Fluid Dynamics (ICCFD3)*, edited by C. Groth and D. W. Zingg, Springer, Berlin, 2006, pp. 681–686.

[2] Mengistu, T., and Ghaly, W., "Aerodynamic Design of Transonic Cascade Using Parallel Computations of Global Optimizers and Artificial Neural Networks," *Computational Fluid Dynamics 2004: Proceedings of the Third International Conference on Computational Fluid Dynamics (ICCFD3)*, edited by C. Groth and D. W. Zingg, Springer, Berlin, 2006, pp. 669–674.

[3] Rumsey, C., Gatski, T., III, Sellers, W., Vatsa, V., and Viken, S., "Summary of the 2004 CFD Validation Workshop on Synthetic Jets and Turbulent Separation Control," 2nd AIAA Flow Control Conference, AIAA Paper 2004-2217, Portland, OR, 2004.

[4] Huang, L., Huang, P., LeBeau, R., and Hauser, T., "Numerical Study of

Blowing and Suction Control," *Journal of Aircraft*, Vol. 41, No. 5, Sept.–Oct. 2004, pp. 1005–1013.

[5] Dannenberg, R. E., and Weiberg, J. A., "Section Characteristics of a 10.5-Percent Thick Airfoil with Area Suction as Affected by Chordwise Distribution of Permeability," NASA Ames Aeronautical Lab., TN 2847, Moffett Field, CA, Dec. 1952.

[6] Suzen, Y., and Huang, P., "Numerical Simulation of Wake Passing on Turbine Cascades," 41st Aerospace Sciences Meeting and Exhibit, Reno, NV, AIAA Paper AIAA-2003-1256, 2003.

[7] Suzen, Y., Huang, P., Volino, R., Corke, T., Thomas, R., Huang, J., Lake, J., and King, P., "A Comprehensive CFD Study of Transitional Flows in Low-Pressure Turbines Under a Wide Range of Operation Conditions," 33rd AIAA Fluid Dynamic Conference, AIAA Paper 2003-3591, 2003.

[8] Suzen, Y., and Huang, P., "Predictions of Separated and Transitional Boundary Layers Under Low-Pressure Turbine Airfoil Conditions Using an Intermittency Transport Equation," *Journal of Turbomachinery*, Vol. 125, No. 3, July 2003, pp. 445–464.

[9] Katam, V., Likki, S., LeBeau, R., and Jacob, J., "Simulation of Separation Control on a Morphing Wing with Conformal Camber," AIAA Fluid Dynamics Conference and Exhibit, Toronto, Canada, AIAA Paper 2005-4880, June 2005.

[10] Katam, V., LeBeau, R., and Jacob, J., "Experimental and Computational Investigation of a Modified NACA 4415 in Low-Re Flows," 22nd Applied Aerodynamics Conference and Exhibit, Providence, RI, AIAA Paper 2004-4972 2004.

[11] Menter, F., "2-Equation Eddy-Viscosity Turbulence Models for Engineering Applications," *AIAA Journal*, Vol. 32, No. 5, 1994, pp. 1598–1605.

[12] Anon., "MPI: A Message-Passing Interface Standard," *International Journal of Supercomputer Applications and High Performance Computing*, Vol. 8, Nos. 3–4, 1994.

[13] Huang, L., LeBeau, R., Huang, P., and Hauser, T., "Optimization of Blowing and Suction Control on a NACA 0012 Airfoil Using Genetic Algorithm," 42nd AIAA Aerospace Sciences Meeting and Exhibit, Reno, NV, AIAA Paper 2004-225, Jan. 2004.

[14] Goldberg, D. E., *Genetic Algorithms in Search, Optimization, and Machine Learning*, Addison Wesley Longman, Reading, MA, 1989, Chap. 5.

[15] Holland, J., *Adaption in Natural and Artificial Systems*, Univ. of Michigan Press, Ann Arbor, MI, 1975.

[16] Huang, L., "Optimization of Blowing and Suction Control on NACA 0012 Airfoil with Diversity Control", Ph.D. Thesis, Dept. of Mechanical Engineering, Univ. of Kentucky, Lexington, KY, 2004.

[17] Oyama, A., Obayashi, S., and Nakahashi, K., "Real-Coded Adaptive Range Genetic Algorithm and Its Application to Aerodynamic Design," *JSME International Journal, Series A (Mechanics and Material Engineering)*, Vol. 43, No. 2, Feb. 2000, pp. 124–129.

[18] Degani, A. T., Li, Q., and Walker, J. D. A., "Unsteady Separation from the Leading Edge of a Thin Airfoil," *Physics of Fluids*, Vol. 8, No. 3, 1996, pp. 704–714.

[19] Rumsey, C., Gatski, T., Sellers, W., Vatsa, V., and Viken, S., "Summary of the 2004 Computational Fluid Dynamics Validation Workshop on Synthetic Jets," *AIAA Journal*, Vol. 44, No. 2, Feb. 2006, pp. 194–207.